

Towards a first-principles theory of surface thermodynamics and kinetics

C. Stampfl,¹ H. J. Kreuzer,² S. H. Payne,² H. Pfnür,³ and M. Scheffler,¹

¹*Fritz-Haber-Institut der Max-Planck-Gesellschaft, Faradayweg 4-6, D-14195 Berlin, Germany*

²*Department of Physics, Dalhousie University, Halifax, Nova Scotia, B3H 3J5, Canada*

³*Institut für Festkörperphysik, Universität Hannover, Appelstrasse 2, D-30176 Hannover, Germany*

Understanding of the complex behavior of particles at surfaces requires detailed knowledge of both macroscopic and microscopic processes that take place; also certain processes depend critically on temperature and gas pressure. To link these processes we combine state-of-the-art microscopic, and macroscopic phenomenological, theories. We apply our theory to the O/Ru(0001) system and calculate thermal desorption spectra, heat of adsorption, and the surface phase diagram. The agreement with experiment provides validity for our approach which thus identifies the way for a predictive simulation of surface thermodynamics and kinetics.

PACSnumbers: 68.45.Da, 82.65.My, 82.65.Dp

The study of the physical and chemical processes that take place at gas-surface interfaces have long been an area of intense research. This interest is both fundamental as well as driven by the possible discovery of important technological applications, e.g. in the field of heterogeneous catalysis, corrosion, etc.^{1,2}. With respect to the field of the *theory* of adsorption of gases on solid surfaces, advancement in recent years has developed in two distinct, albeit complimentary directions: (i) electronic structure calculations, at best done by density-functional theory (DFT), to determine the geometries, energetics, and vibrational properties of adsorbate covered surfaces, and (ii) phenomenological models, both for the thermodynamics and the kinetics³ of the adsorbate. If one can assume that the geometry of the solid surface does not change dramatically and that adsorption occurs at well defined sites, one frequently employs a lattice gas model. A number of parameters enter such a model such as the binding energies and vibrational frequencies of a single adparticle in the various adsorption sites, and their mutual lateral interactions with adparticles in close-by sites. Traditionally, these parameters are adjusted in the theory to fit a variety of experimental data such as phase diagrams, heats of adsorption, infrared spectra and thermal desorption data, etc. Such an approach, while useful, is clearly not necessarily predictive in nature, nor the parameters unique, and may not capture the physics of the microscopic processes that are behind the “best-fit” adjusted “effective” parameters.

In the present letter, with the aim to improve upon this approach, we combine state-of-the-art procedures of (i) microscopic theories, i.e. DFT electronic structure calculations and (ii) macroscopic phenomenological approaches, i.e. lattice gas and rate equations, and Monte Carlo schemes. On doing this, we present a consistent first-principles based approach for calculation of the thermodynamic and kinetic properties of an adsorbate, such as heats of adsorption, temperature programmed desorption (TPD) spectra, and the surface phase diagram. We have chosen the system of oxygen at Ru(0001) for which detailed structural⁴⁻⁹, thermodynamic¹⁰, and kinetic data^{11,12} exist. We will show that with the present approach, a realistic description of these physical properties is indeed feasible.

We like to mention that use of results of *ab initio* electronic structure calculations as input to statistical mechanical computer codes have also been developed for the description of bulk alloy phase diagrams^{13,14} and island growth on crystal surfaces¹⁵. To our knowledge, however, there has been no application of such an approach for the processes that we are interested in here.

The electronic structure calculations¹⁶ are performed using DFT and the generalized gradient approximation (GGA) for the exchange-correlation functional¹⁷ (hereafter denoted as DFT-GGA). We use the pseudopotential^{18,19} plane wave method and the supercell approach to model the surface. The position of the O atoms and the top two Ru layers are fully relaxed. The DFT-GGA Ru pseudopotential yields a bulk hcp-fcc energy difference of ≈ -0.072 eV in good agreement with all-electron calculations.²⁰ For further details we refer to Refs.^{6,21}

To set up a lattice gas model for O on Ru(0001) we require a hamiltonian, which we express as:

$$\begin{aligned}
 H = & E_s^{\text{hcp}} \sum_i n_i + E_s^{\text{fcc}} \sum_i n_i + \frac{1}{2} (V_{1n}^{\text{hcp}} \sum_{i,a} n_i n_{i+a} \\
 & + V_{1n}^{\text{fcc}} \sum_{i,a} n_i n_{i+a} + V_{1n}^{\text{hcp-fcc}} \sum_{i,a'} n_i n_{i+a'} \\
 & + V_{2n}^{\text{hcp}} \sum_{i,b} n_i n_{i+b} + V_{2n}^{\text{fcc}} \sum_{i,b} n_i n_{i+b} \\
 & + V_{2n}^{\text{hcp-fcc}} \sum_{i,b'} n_i n_{i+b'} + V_{3n}^{\text{hcp}} \sum_{i,c} n_i n_{i+c} \\
 & + V_{3n}^{\text{fcc}} \sum_{i,c} n_i n_{i+c} + V_{3n}^{\text{hcp-fcc}} \sum_{i,c'} n_i n_{i+c'} \\
 & + V_{\text{trio}}^{\text{hcp}} \sum_{i,a,a'} n_i n_{i+a} n_{i+a'} + V_{\text{trio}}^{\text{fcc}} \sum_{i,a,a'} n_i n_{i+a} n_{i+a'} + \dots)
 \end{aligned} \tag{1}$$

The different unit cells of the substrate surface are labeled by an index i with $i+a$, etc. labeling neighboring cells, and we introduce occupation numbers $n_i = 0$ or 1 depending on whether a site in cell i is empty or occupied. Overcounting of cells is excluded in the summations. Eq. 1 includes consideration of hcp and fcc sites. The indices a' , b' , and c' indicate that the first, second, and third neighbor distances between atoms in hcp and fcc sites are different to when they occupy the same type of sites. Here $E_s^{\text{hcp}} = |V_0| - k_B T \ln q_3$ is the binding energy of an isolated particle in an hcp site. $|V_0|$ is the depth of the adsorption potential with reference to the energy of a gas phase molecule which adsorbs dissociatively. q_3 is the partition function of the atom accounting for its vibration perpendicular, and its frustrated trans-

lation parallel, to the surface. V_{1n}^{hcp} , V_{2n}^{hcp} and V_{3n}^{hcp} are the first, second and third neighbor interaction energies between two adsorbed O atoms in hcp sites. The analogous terms labeled “fcc” represent the same quantities but for adsorption in fcc sites. Terms labeled $V^{\text{hcp-fcc}}$ represent the interactions between atoms in hcp and fcc sites. Trio (and higher cluster) interaction energies, V_{trio} , account for additional modifications because the interaction between two adsorbed O atoms is changed, when a third adatom is close by. In fact, depending on the angles and distances, there are three different trio interactions taken into account.

We determine the lateral interaction energies required in Eq. 1 from DFT-GGA calculations of ordered structures of O on Ru(0001) (see Fig. 1). The adsorption energy of a *single* oxygen atom on Ru(0001) is obtained using a (3×3) structure with coverage $\theta = 1/9$. With this large O-O separation (8.26 Å), which corresponds to the fifth nearest neighbor distance of alike sites, lateral interactions are negligible. The adsorption energy, with respect to $1/2\text{O}_2$, is then expressed as,

$$E_a^{\theta=1/9} = E_{\text{total}}^{\text{O/Ru}} - E_{\text{total}}^{\text{Ru}} - 1/2E_{\text{total}}^{\text{O}_2} \quad (2)$$

Here $E_{\text{total}}^{\text{O/Ru}}$, $E_{\text{total}}^{\text{Ru}}$, and $E_{\text{total}}^{\text{O}_2}$ are the total energies of the (3×3) -O/Ru(0001) system, the clean Ru surface, and a free O_2 molecule, respectively. Expressions analogous to Eq. 2 have been used to derive the adsorption energies for the other coverages (see Tab. I). We expand the adsorption energies in terms of two- and three-body interactions. The interaction parameters are derived from the equations:

$$\begin{aligned} E_a^{\theta=2/9} &= V_0 + \frac{1}{2}(V_{1n} + V_{3n}) \\ E_a^{\theta=1/4} &= V_0 + 3V_{3n} \\ E_a^{\theta=1/3} &= V_0 + 3V_{2n} \\ E_a^{\theta=1/2} &= V_0 + V_{1n} + V_{2n} + 3V_{3n} + V_{1t} \\ E_a^{\theta=2/3} &= V_0 + \frac{3}{2}V_{1n} + 3V_{2n} + \frac{3}{2}V_{3n} + 3V_{bt} \\ E_a^{\theta=3/4} &= V_0 + 2V_{1n} + 2V_{2n} + 3V_{3n} + 2V_{1t} + 2V_{bt} + \frac{2}{3}V_{tt} \\ E_a^{\theta=1.0} &= V_0 + 3(V_{1n} + V_{2n} + V_{3n}) + 3V_{1t} + 6V_{bt} + 2V_{tt} \end{aligned}$$

where V_{1t} , V_{bt} and V_{tt} are linear, bent and triangular trios, respectively (indicated in Fig. 1). We point out that only in the (3×3) -2O structure at $\theta = 2/9$ can the atoms at nearest neighbor sites move significantly from the locally 3-fold symmetric adsorption sites to reduce the repulsion, V_{1n} . However, with strong nearest neighbor repulsion, isolated nearest neighbor pairs are highly improbable at any coverage.

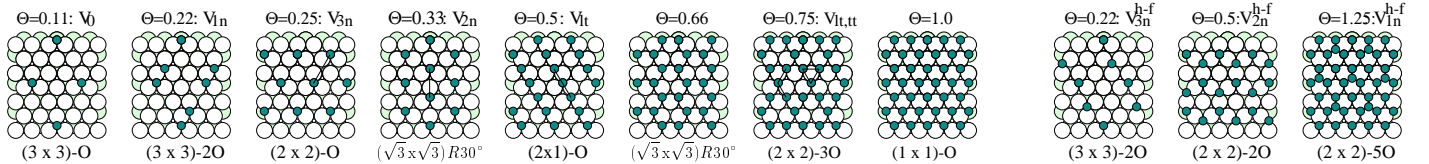


FIG. 1. Adsorbate structures calculated using DFT-GGA. (For the first eight diagrams analogous calculations were also performed for O in fcc sites.) Small circles represent O atoms and large circles Ru atoms.

We have therefore calculated $E_a^{\theta=2/9}$ for atoms at locally 3-fold symmetric sites because if we were to use the relaxed structure we would need to include higher many-body interactions (e.g. longer-ranged trios, quartos and quintos etc.) to account for the movement of the atoms back to the ideal 3-fold sites which occurs for higher coverages.

We thus have for O atoms in hcp sites (and analogously for O atoms in fcc sites) seven equations for six unknowns. Using the first six of these equations we obtain the interaction energies listed in Tab. II. The accuracy of these interaction values is gauged by calculating the adsorption energy of the monolayer (seventh equation); we find a discrepancy of 0.034 eV smaller than that of the DFT-GGA value. Along with our derived values in Tab. II, we give in brackets the interaction energies determined by Piercy *et al.*¹⁰ for their best-fit to the experimental O/Ru(0001) phase diagram. We also include our derived interaction parameters for structures involving O atoms in hcp and fcc sites (last three diagrams of Fig. 1) obtained by writing down appropriate equations in an analogous manner to those listed above.

To complete the specification of our hamiltonian, we need the vibrational frequencies of an O atom relative to the Ru surface. These frequencies can also be calculated using density-functional theory. For example, we obtain for the vibration of oxygen normal to the surface (at the $\bar{\Gamma}$ -point) $\nu_z = 509 \text{ cm}^{-1}$. The experimental value is 535 cm^{-1} (for O in the (2×2) phase)²².

We now proceed to calculate the temperature programmed thermal desorption spectra. Writing the kinetic equation for adsorption and desorption as $d\theta/dt = R_{\text{ad}} - R_{\text{des}}$, we obtain for an atomic adsorbate in contact with a gas of diatomic homonuclear molecules, the rate of adsorption $R_{\text{ad}} = 2S_{\text{dis}}(\theta, T)P_m a_s \lambda_m / h$. Here P_m is the molecular pressure above the surface, a_s is the area of one unit cell of the substrate surface, $\lambda_m = h / (2\pi m k_B T)^{1/2}$ is the thermal wavelength of a molecule of mass m , and $S_{\text{dis}}(\theta, T)$ is the dissociative sticking coefficient. For the rate of desorption we have³,

$$R_{\text{des}} = 2S_{\text{dis}}(\theta, T) a_s \frac{k_B T}{h \lambda_m^2} \frac{Z_{vr}}{q_3^2} \frac{\theta^2}{(1-\theta)^2} e^{\frac{-2|V_0|}{k_B T}} e^{\frac{2\mu^{(\text{lat})}}{k_B T}} \quad (3)$$

Here Z_{vr} is the partition function accounting for the internal vibrations and the rotations of O_2 in the gas phase. $\mu^{(\text{lat})}$ is the contribution to the chemical

potential of the adsorbate due to the lateral interactions in the hamiltonian (Eq. 1) and is calculated here using transfer matrix techniques. Regarding the sticking coefficient, we note that dissociation is not activated initially, but at (local) coverages of $\theta \gtrsim 0.5$, it is hindered by an energy barrier^{6,12}. Under these circumstances, to obtain the coverage and temperature dependence of the sticking coefficient *ab initio* would be a significant undertaking. Therefore we use an analytic expression which well approximates the measured behavior in the temperature regime of desorption¹²: The sticking coefficient drops approximately as $(2/3 - \theta)^2$ and for coverages above $2/3$ it remains very small up to a monolayer. The actual equation we use is: $S_{\text{dis}}(\theta) = S_0 \exp[-(\theta/\sigma)^2]$, with $S_0=0.27$ and $\sigma=0.3$.

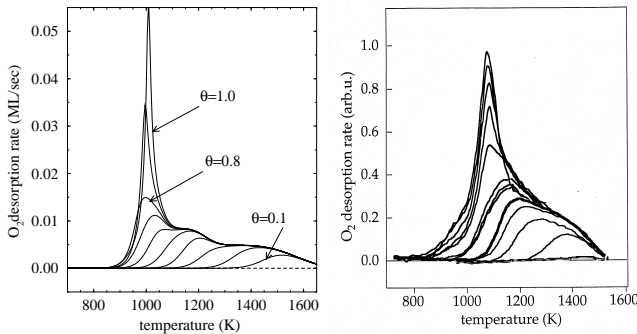


FIG. 2. Theoretical (left panel) and experimental²⁴ (right panel) TPD spectra (heating rate of 6 K/s). For the theoretical results initial coverages are $\Theta = 0.1$ to 1.0 in steps of 0.1; the experimental results also span the initial coverage region of $\theta \rightarrow 0$ to 1ML.

Our calculated TPD spectra²³ are shown in Fig. 2 which are compared to recent experimental data²⁴. For low initial coverage we note that in the theory the oxygen desorbs at about 100 K higher temperature than in experiment, reflecting an overbinding of the O atoms. We believe that this size of error is typical for present day state-of-the-art calculations and don't see that (or how) better accuracy will be achieved in the coming five to ten years. Aside from this, it can be seen that the theoretical spectra exhibit all the features of the experimental data: (i) a shift of the peak maxima to lower temperatures for higher initial coverages (appropriate for second order desorption and/or for repulsive interactions) and (ii) a steepening of the leading edge for higher initial coverages. In our theory this steepening is a reflection of two facts: Firstly, for increasing coverages, the repulsive

Site	$V_0 = E_a^{\theta=1/9}$	$E_a^{\theta=2/9}$	$E_a^{\theta=1/4}$	$E_a^{\theta=1/3}$	$E_a^{\theta=1/2}$	$E_a^{\theta=2/3}$	$E_a^{\theta=3/4}$	$E_a^{\theta=1}$	Site	$E_{a,\text{hcp-fcc}}^{\theta=2/9}$	$E_{a,\text{hcp-fcc}}^{\theta=1/2}$	$E_{a,\text{hcp-fcc}}^{\theta=5/4}$
hcp	-2.503	-2.417	-2.577	-2.370	-2.307	-2.150	-2.091	-1.895	hcp-fcc	-2.294	-2.209	-1.492
fcc	-2.152	-2.107	-2.145	-2.105	-2.025	-2.015	-1.942	-1.865				

TABLE I. Adsorption energies (in eV) for O on Ru(0001) with respect to $1/2\text{O}_2$ for various coverages.

next nearest neighbor interactions lower the binding energy and thus lower the onset of desorption, broadening the TPD spectra and steepening the rising edge; secondly, and more importantly, is the effect of the rapidly decreasing sticking probability for increasing coverage²⁵. Because the sticking coefficient is much smaller for coverages above $2/3\text{ML}$, desorption is delayed to higher temperatures and the last third of a monolayer desorbs over a very narrow temperature range. If we use the ideal dissociative sticking, $S(\theta) = S_0(1 - \theta)^2$, a similar steepening still occurs but the onset of desorption occurs 100 K earlier at a monolayer. A similar behavior has been discussed in Ref.²⁵. We can trace the two shoulders (at 1100K and 1300K) to the synergy of the interactions that at lower temperatures lead to the formation of the (2×1) and (2×2) ordered structures which will also be seen in the heat of adsorption.

Piercy *et al.*¹⁰ find that to obtain a satisfactory explanation of the *surface phase diagram* in the vicinity of the order-disorder transition temperature, a spillover into fcc sites of about 12 % takes place. In the temperature regime of desorption, localization in hcp sites should be even less. We find, however, that the overall features of the TPD spectra remain essentially unchanged whether spillover is included or not. We have also tested the importance of the trio interactions on desorption. Neglecting them increases the overall repulsion for coverages larger than $2/3\text{ ML}$ and consequently broadens the TPD spectra, reducing the agreement with experiment. We therefore conclude that for high O-coverages trio interactions play an important role.

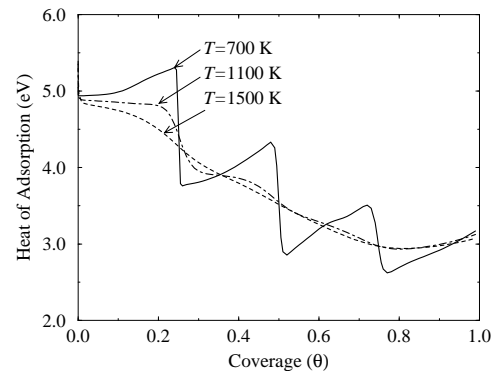


FIG. 3. The heat of adsorption as a function of coverage for temperatures of $T=700\text{ K}$ (sharpest features), 1100 K, and 1500 K.

Having the chemical potential as a function of temperature and coverage, we can also calculate the equilibrium properties of the adsorbate, such as adsorption isobars. As an example, we present in Fig. 3 the isosteric heat of adsorption³ for a few temperatures. At the highest temperature a smooth decrease is observed. At the lowest temperature, sharp peaks (and decreases) at 1/4, 1/2, 3/4, and 1 ML occur. These coverages correspond to each of the ordered phases that form *in nature*, i.e. (2×2) -O⁴, (2×1) -O⁵, (2×2) -3O⁷⁻⁹, and (1×1) -O⁶. (Note that the existence of the (2×2) -3O, and (1×1) -O adsorption phases was at first predicted by DFT-GGA calculations²¹ and subsequently confirmed by experiment; a nice success of DFT.) The rises in between originate from the third neighbor attractions, and also from the trios for the higher coverages. Our results show no tendency for the stability of a $\theta = 1/3$ phase, i.e. a $(\sqrt{3} \times \sqrt{3})R30^\circ$ structure, in agreement with experiment. We now turn to the surface phase diagram. From Tab. II it can be seen that the overall agreement of the interaction parameters determined from our density-functional calculations and from the best-fit to experiment in Ref.¹⁰ is, in general, astonishingly good; but there are some significant differences (i.e. more than 50% for V_{1n}^{fcc}) which could be expected. We find that our Monte Carlo simulations yields a surface phase diagram rather similar to that of Piercy *et al.*¹⁰ where coverage up to half a monolayer was considered. Our present simulations also included higher O coverages and correctly predict formation of the (2×2) -3O phase.

In summary, we have presented a first-principles based approach for calculation of the thermodynamics and kinetics of an adsorbate on a surface. We used density-functional theory to create a lattice gas hamiltonian from which we evaluated the partition function. Our theoretical temperature programmed thermal desorption spectra, heats of adsorption, and the surface phase diagram for O on Ru(0001) show very good overall agreement with available experimental results, providing confidence in our approach. We found that trio interactions, as well as the sticking coefficient, play an important role in the TPD spectra of the present system. The attractive trio interactions also apparently help stabilize the higher coverage (2×1) -O, (2×2) -3O, and (1×1) -O phases. The affect of spillover into fcc sites was found to have a minimal affect on the TPD spectra.

Site	V_{1n}	V_{2n}	V_{3n}	V_{1t}	V_{bt}	V_{tt}
hcp	0.265 (0.23)	0.044 (0.069)	-0.025 (-0.023)	-0.039	-0.046	0.058
fcc	0.158 (0.069)	0.016	0.002	-0.052	-0.044	0.076
fcc-hcp	0.586	0.101	0.033			

TABLE II. DFT-GGA calculated interaction energies (in eV) Piercy *et al.*¹⁰.

-
- ¹ *The chemical physics of solid surfaces and heterogeneous catalysis*, eds. D. A. King and D. P. Woodruff, Studies in Surface Science and Catalysis, Vol. 4, Elsevier, Amsterdam (1982).
 - ² *Equilibria and dynamics of gas adsorption on heterogeneous solid surfaces*, eds. W. Rudziński, W. A. Steele, and G. Zgrablich, Vol. 104, Elsevier (1997).
 - ³ H.J. Kreuzer and S.H. Payne, in Ref. [2].
 - ⁴ M. Lindroos, H. Pfnür, D. Held, D. Menzel, Surf. Sci. **222**, 451 (1989).
 - ⁵ H. Pfnür, D. Held, M. Lindroos, D. Menzel, Surf. Sci. **220**, 43 (1989).
 - ⁶ C. Stampfl, S. Schwegmann, H. Over, M. Scheffler, and G. Ertl, Phys. Rev. Lett. **77**, 3371 (1996).
 - ⁷ K. L. Kostov, M. Gsell, P. Jakob, T. Moritz, W. Widdra, and D. Menzel, Surf. Sci. **394**, L138 (1997).
 - ⁸ Y. D. Kim, S. Wendt, S. Schwegmann, H. Over, and G. Ertl, Surf. Sci. **418**, 267 (1998).
 - ⁹ M. Gsell, M. Stichler, P. Jakob, and D. Menzel, Israel J. Chem. **38**, 339 (1999).
 - ¹⁰ P. Piercy, K. De'Bell, H. Pfnür, Phys. Rev. B **45**, 1869 (1992).
 - ¹¹ T. E. Madey, H. A. Engelhardt, and D. Menzel, Surf. Sci. **48**, 304 (1975).
 - ¹² L. Surnev, G. Rangelov, and G. Bliznakov, Surf. Sci. **159**, 299 (1985).
 - ¹³ D. de Fontaine, Solid State Phys. **47**, 33 (1994).
 - ¹⁴ A. Zunger, in *Statics and Dynamics of Alloy Phase Transformations*, eds. P. E. A. Turchi and A. Gonis, NATO ASI Series, Plenum Press, New York (1994) p 361.
 - ¹⁵ P. Ruggerone, C. Ratsch, and M. Scheffler, in *Growth and Properties of Ultrathin Epitaxial Layers*, eds. D.A. King, D.P. Woodruff. The Chemical Physics of Solid Surfaces, Vol. 8. Elsevier Science, Amsterdam (1997), p 490.
 - ¹⁶ R. Stumpf and M. Scheffler, Comput. Phys. Commun. **79**, 447 (1994); M. Bockstedte, A. Kley, J. Neugebauer, and M. Scheffler, Comput. Phys. Comm. **107**, 187 (1997).
 - ¹⁷ J. P. Perdew, J. A. Chevary, S. H. Vosko, K. A. Jackson, M. R. Pederson, D. J. Singh, and C. Fiolhais, Phys. Rev. B **46**, 6671 (1992).
 - ¹⁸ N. Troullier and J. L. Martins, Phys. Rev. B **43**, 1993 (1991).
 - ¹⁹ M. Fuchs and M. Scheffler, Comput. Phys. Commun., **119**, 67 (1999).
 - ²⁰ H. L. Skriver, Phys. Rev. B **31**, 1909 (1985).
 - ²¹ C. Stampfl and M. Scheffler, Phys. Rev. B **54**, 2868 (1996); Surf. Sci., **377-379**, 808 (1997).
 - ²² T. S. Rahman, A. B. Anton, N. R. Avery, and W. H. Weinberg, Phys. Rev. Lett. **51**, 1979 (1983).
 - ²³ ASTEK package written by H. J. Kreuzer and S. H. Payne (available from Helix Science Applications, Box 49, Site 3, R.R.5, Armdale NS, B3L 455 Canada).
 - ²⁴ A. Böttcher, H. Niehus, S. Schwegmann, H. Over, and G. Ertl, J. Phys. Chem. **101**, 11185 (1997).
 - ²⁵ F. Buatier de Mongeot, M. Rocca, A. Cupolillo, U. Valbusa, H.J. Kreuzer, S.H. Payne, J. Chem. Phys. **106**, 711 (1997).